HHS Public Access

Author manuscript

Sci Immunol. Author manuscript; available in PMC 2021 November 09.

Published in final edited form as:

Sci Immunol. 2021 March 05; 6(57): . doi:10.1126/sciimmunol.abe3218.

The ChAT-acetylcholine pathway promotes group 2 innate lymphoid cell responses and anti-helminth immunity

Coco Chu[1], **Christopher N. Parkhurst**[1,†], **Wen Zhang**[1,†], **Lei Zhou**[1], **Hiroshi Yano**[1], **Mohammad Arifuzzaman**[1], **David Artis**[1,2,*]

[1]Jill Roberts Institute for Research in Inflammatory Bowel Disease, Joan and Sanford I. Weill Department of Medicine, Department of Microbiology and Immunology, Weill Cornell Medicine, Cornell University, New York, NY 10021, USA

[2]Friedman Center for Nutrition and Inflammation, Joan and Sanford I. Weill Department of Medicine, Department of Microbiology and Immunology, Weill Cornell Medicine, Cornell University, New York, NY 10021, USA

Abstract

Group 2 innate lymphoid cells (ILC2s) reside in multiple tissues including lymphoid organs and barrier surfaces, and secrete type 2 cytokines including interleukin (IL)-5, IL-9 and IL-13. These cells participate in multiple physiological processes including allergic inflammation, tissue repair, metabolic homeostasis and host defense against helminth infections. Recent studies indicate that neuropeptides can play an important role in regulating ILC2 responses, however, the mechanisms that underlie these processes *in vivo* remain incompletely defined. Here, we identify that activated ILC2s upregulate choline acetyltransferase (ChAT)—the enzyme responsible for the biosynthesis of acetylcholine (ACh)—following infection with the helminth parasite *Nippostrongylus brasiliensis* or treatment with alarmins or cytokines including IL-25, IL-33 and thymic stromal lymphopoietin (TSLP). ILC2s also express acetylcholine receptors (AChRs), and ACh administration promotes ILC2 cytokine production and elicits expulsion of helminth infection. In accordance with this, ChAT deficiency in ILC2s leads to defective ILC2 responses and impaired immunity against helminth infection. Together, these results reveal a previously unrecognized role of the ChAT-ACh pathway in promoting type 2 innate immunity to helminth infection.

One Sentence Summary:

*Corresponding author. dartis@med.cornell.edu.

†These authors contributed equally to this work.

Author contributions: C.C. carried out most of the experiments and analyzed the data. C.N.P., W.Z., L.Z., H.Y. and M.A. helped with experiments. D.A. and C.C. conceived the project, analyzed data, and wrote the manuscript with input from all co-authors.

Competing interests: D.A. has contributed to scientific advisory boards at Genentech, Pfizer, Takeda, FARE, and the KRF. The other authors declare no competing interests.

Data and materials availability: RNA-seq data are available at Gene Expression Omnibus under accession numbers GSE164705. All datasets generated and/or analyzed during the current study are present in the paper or the Supplementary Materials or are available from the corresponding author upon reasonable request.

Note added in proof: A similar study by Roberts et al. reports a critical role for ILC2-derived ACh in promoting type 2 inflammation (60).

Activated ILC2s utilize the ChAT-acetylcholine pathway to enhance their cytokine production and promote helminth expulsion.

Introduction

Group 2 innate lymphoid cells (ILC2s) are potent producers of type 2 cytokines, including interleukin (IL)-5, IL-9 and IL-13, and participate in a wide range of physiological processes, including tissue homeostasis and repair, type 2 inflammation, metabolic homeostasis and anti-helminth immunity (1–7). In addition to activation by cytokines and environmental factors, recent studies indicate that multiple neurotransmitters and neuropeptides are key regulators of divergent ILC2 responses (8–10), highlighting the close association between the nervous system and innate immunity at barrier surfaces.

For example, a subset of cholinergic neurons express the neuropeptide neuromedin U (NMU), directly activate ILC2s through the NMU receptor 1 (NMUR1), induce ILC2 proliferation and type 2 cytokine production, and accelerate helminth expulsion. However, NMU-activated ILC2s can also promote allergic inflammation under certain circumstances (11–13). In contrast, adrenergic neurons express the neurotransmitter norepinephrine (NE), inhibiting ILC2 responses, type 2 inflammation and helminth expulsion through binding to β2-adrenergic receptors (β_2AR) on ILC2s (14). In addition, another neuropeptide calcitonin gene-related peptide (CGRP) binds to its receptor CALCRL/RAMP1, which is expressed in a subpopulation of ILC2s, antagonizing ILC2 activation, proliferation and cytokine production, and suppressing allergic inflammation and anti-helminth immunity (15–17). Nociceptor neurons (18, 19) and a subset of cholinergic neurons (15) can produce CGRP, as well as a subset of ILC2 themselves during inflammation (15–17), creating a negative feedback loop in type 2 innate immune responses. Moreover, ILC2s upregulate the expression of tryptophan hydroxylase 1 (Tph1, the rate-limiting enzyme in serotonin biosynthesis) upon activation with IL-33 and can secrete serotonin, and conditional deletion of Tph1 in lymphocytes results in increased susceptibility to helminth infection (20). However, whether ILC2s secrete other neurotransmitters or neuropeptides and potentially form a regulatory feedback loop to control ILC2 responses is unknown.

Acetylcholine (ACh) was the first neurotransmitter discovered in 1921 (21, 22). It is synthesized from the compounds choline and acetyl coenzyme A by the enzyme choline acetyltransferase (ChAT). ACh acts on two families of receptors—nicotinic acetylcholine receptors (nAChRs) and muscarinic acetylcholine receptors (mAChRs), both named by their agonists—nicotine and muscarine. nAChRs are pentameric Na^+ ion channels, and their activation results in Na^+ influx and excitation of the neuron (23). mAChRs are G-protein coupled receptors and contain five subtypes (M1–5). M1, M3, and M5 receptors are generally coupled to $G_{q/11}$ proteins to perform stimulatory functions, while M2 and M4 receptors are coupled to $G_{i/o}$ proteins, leading to inhibitory effects (24). ACh in the nervous system works at neuronal synapses and neuromuscular junctions, mediating communication between neurons as well as neural communication to the muscles. The action of acetylcholine is terminated by acetylcholinesterase (AChE) (25). Notably, parasitic helminths such as *N. brasiliensis*, are known to express AChE throughout its life cycle (26,

27), suggesting this may be a mechanism of immune evasion employed by this group of pathogens. However, whether the ChAT-ACh pathway plays a role in protective immunity against helminth infection has not been defined.

In this study, we demonstrate that activated ILC2s upregulate ChAT expression in both lymphoid organs and mucosal tissues following *N. brasiliensis* infection or after treatment with alarmins or cytokines including IL-25, IL-33 and thymic stromal lymphopoietin (TSLP). ILC2s express several AChRs, which are also regulated by IL-25 and IL-33. In addition, treatment with ACh leads to elevated ILC2-derived IL-5 and IL-13 production both *in vitro* and *in vivo*, and enhanced eosinophil and goblet cell responses and accelerated expulsion of *N. brasiliensis in vivo*. In accordance with this, conditional deletion of ChAT in ILC2s results in defective cytokine production, impaired type 2 inflammation and delayed protective immunity to *N. brasiliensis* infection. Together, these results reveal a previously unrecognized non-neuronal source of ACh that regulates ILC2 effector function, and define a critical role for the ChAT-ACh pathway in promoting innate immunity and host defense against helminth infection.

Results

ILC2s up-regulate ChAT expression following helminth infection

ILC2s play a critical role in promoting innate immunity against helminth infection (1, 3–6, 28–31). To study the role of the ChAT-ACh pathway in regulating ILC2 responses following helminth infection, we first infected ChAT^{BAC}-eGFP reporter mice (32) with *N. brasiliensis*, and analyzed the expression of *Chat*-eGFP in ILC2s by flow cytometry. In naive mice, ILC2s expressed very low levels of *Chat*-eGFP (Fig. 1, A to F). However, following *N. brasiliensis* infection, ILC2s up-regulated *Chat*-eGFP expression, and there were significantly higher percentages and numbers of *Chat*-eGFP$^+$ ILC2s in multiple organs, including the lung and mesenteric lymph nodes (mLNs) of *N. brasiliensis*-infected mice compared to uninfected mice (Fig. 1, A to F). We confirmed the *Chat* mRNA expression in *Chat*-eGFP$^+$ ILC2s by quantitative PCR (qPCR) and RNA-sequencing (RNA-seq) (fig. S1, A to C). In addition, *Chat*-eGFP expression was negatively associated with the expression of both ST2 (IL-33 receptor) and CD25 in ILC2s (fig. S1, D to G). In accordance with this, the majority of ChAT$^+$ ILC2s were inflammatory ILC2s, which are elicited following helminth infection and phenotypically have low expression of ST2 and CD25, rather than natural ILC2s which have high expression of these two markers (Fig. 1, G and H). Moreover, ILC2s exhibited a significantly higher frequency of *Chat*-eGFP$^+$ cells compared to other cell types, including ILC1s, ILC3s, CD4$^+$ T cells, CD8$^+$ T cells, B cells, NK cells, eosinophils, macrophages and neutrophils (fig. S1, H and I).

We also employed immunofluorescence microscopy to visualize *Chat*-eGFP$^+$ ILC2s in the small intestine, as well as in the lung and mLNs of uninfected and *N. brasiliensis*-infected mice. Consistent with the flow cytometry data, ILC2s up-regulated *Chat*-eGFP expression after *N. brasiliensis*-infection as observed in the small intestinal lamina propria, lung parenchyma and mLNs (Fig. 2, A to F, and fig. S2, A to F), indicating that the ChAT-ACh pathway may participate in ILC2-mediated host defense against helminth infection.

ILC2s up-regulate ChAT expression following IL-33 treatment

The alarmin cytokine, IL-33, is constitutively expressed in the nuclei of intestinal epithelial cells, endothelial cells and fibroblasts, as well as in mast cells, macrophages and dendritic cells during inflammation (2, 33), and in stromal cells of white adipose tissues (34, 35). When the small intestinal barrier is breached by *N. brasiliensis*, IL-33 is released by stressed or damaged intestinal epithelial cells, directly acts on the IL-33 receptor complex expressed on ILC2s, and is a key activator of ILC2-dependent innate immune responses against *N. brasiliensis* infection (2, 36, 37). To test whether IL-33 can directly affect ChAT expression in ILC2s, we sort-purified ILC2s from the small intestinal lamina propria of ChAT^{BAC}-eGFP reporter mice, cultured them *in vitro* with or without IL-33, and analyzed the expression of *Chat*-eGFP by flow cytometry. Notably, ILC2s cultured in the presence of IL-33 exhibited significantly higher percentage of *Chat*-eGFP^{+} cells as well as higher *Chat*-eGFP level (measured by MFI) compared to ILC2s cultured with IL-2 and IL-7 alone (Fig. 3, A to C). Consistent with the *in vitro* data, intraperitoneal administration of IL-33 significantly enhanced the percentages and numbers of *Chat*-eGFP^{+} ILC2s in multiple organs of ChAT^{BAC}-eGFP reporter mice, including the small intestine, lung, mLNs and colon (Fig. 3, D to I, and fig. S3, A to F). Moreover, after IL-33 treatment, elevated *Chat*-eGFP^{+} ILC2 responses were observed in the small intestinal lamina propria, lung parenchyma, mLNs and colon of ChAT^{BAC}-eGFP reporter mice by immunofluorescence microscopy compared to untreated mice (fig. S2, A to H, and fig. S4, A and H). Taken together, these results suggest that the alarmin cytokine IL-33 can up-regulate ChAT expression in ILC2s.

To test whether other alarmins or cytokines also regulate ChAT expression in ILC2s, we treated ChAT^{BAC}-eGFP reporter mice with IL-25 or TSLP intraperitoneally, and found that both IL-25 and TSLP significantly increased the percentages of *Chat*-eGFP^{+} ILC2s in the mLNs, with a stronger effect in IL-25-treated mice compared to TSLP-treated mice (Fig. 3J). To test whether other models of type 2 inflammation also regulate ChAT expression in ILC2s, we infected ChAT^{BAC}-eGFP reporter mice with the helminth *Trichuris muris (T. muris)* intragastrically or treated them with the allergen *Alternaria* intranasally, and found significantly higher percentages of *Chat*-eGFP^{+} ILC2s in the cecum of *T. muris*-infected mice compared to uninfected mice, as well as significantly higher percentages of *Chat*-eGFP^{+} ILC2s in the lung of *Alternaria*-treated mice compared to naïve mice (Fig. 3K and L). These data suggest that following exposure to helminths or allergens that trigger the release of IL-25, IL-33 or TSLP, the significant increase in ChAT expression in ILC2s in multiple tissues and organs is a conserved response to multiple stimuli.

ILC2s express acetylcholine receptors

Previous studies identified the expression and function of AChR subunits in immune cell populations, such as α7-nAChR in macrophages and α9-nAChR in B cells (38, 39). To examine whether ILC2s express AChR subunits, first we screened the expression of all 21 AChR subunits in cultured small intestinal ILC2s by reverse transcription PCR (RT-PCR). Notably, ILC2s express *Chrm4* and *Chrm5*, which are G-protein-coupled muscarinic receptors, as well as the α subunits – *Chrna2*, *Chrna5*, *Chrna9*, *Chrna10*, and the β subunits – *Chrnb1* and *Chrnb2*, which form pentameric nicotinic ligand-gated channels (Fig. 4, A to D, and fig. S5, A to D). We confirmed the expression of these candidate AChRs in *ex vivo*

sorted small intestinal ILC2s and lung ILC2s by qPCR or in cultured ILC2s by Western blot (Fig. 4E and fig. S5, E and F). To test whether IL-25 or IL-33 directly regulate the expression of these candidate AChRs in ILC2s, we employed qPCR and compared their expression in cultured ILC2s with or without treatment with IL-25 or IL-33 compared to ILC2s cultured with IL-2 and IL-7 alone. Both IL-25 or IL-33 stimulation promoted the expression of *Chrm4*, and inhibited the expression of *Chrm5*, *Chrna2*, *Chrna10* and *Chrnb2*. However, IL-25 promoted the expression of *Chrna5*, *Chrna9* and *Chrnb1*, while IL-33 inhibited the expression of these three AChRs (Fig. 4, F to M). Collectively, these data indicate that AChRs are expressed on ILC2s and their expression levels are selectively regulated by IL-25 versus IL-33.

ACh promotes ILC2 cytokine production in vitro

To investigate whether ACh directly activates ILC2s, we sorted small intestinal ILC2s and incubated them in media with or without ACh for 4 hours *in vitro* in the presence of IL-2, IL-7, IL-25 and IL-33. We found ACh potently activated ILC2s as measured by intracellular cytokine staining of IL-5 and IL-13 (Fig. 5, A to D). To investigate whether ACh alone activates ILC2s, we sorted small intestinal ILC2s from YetCre-13 (IL-13-YFP reporter) mice (6), incubated them in media with or without ACh for 4 hours *in vitro* and observed that treatment with ACh alone could significantly activate ILC2s as measured by IL-13-YFP expression (Fig. 5, E and F), although to a greater extent when IL-2, IL-7, IL-25 and IL-33 were present (Fig. 5, G and H). Moreover, both ipratropium bromide (a pan mAChR antagonist) and d-tubocurarine (a pan nAChR antagonist) inhibited the effects of ACh on ILC2 IL-13-YFP expression (Fig. 5, I and J), suggesting that ACh may act through both mAChRs and nAChRs expressed on ILC2s to promote cytokine production.

ACh stimulates ILC2s in vivo *and promotes helminth expulsion*

To investigate whether ACh regulates ILC2-mediated innate immunity against *N. brasiliensis* infection *in vivo*, we administered ACh to *N. brasiliensis*-infected mice, and examined the ILC2 responses at 7 days post-infection. Control mice infected with *N. brasiliensis* exhibited typical ILC2 responses as expected, with IL-5 and IL-13 production (Fig. 6, A to G), and subsequent eosinophil recruitment (Fig. 6, H to L) and goblet cell hyperplasia (Fig. 6, M and N). Notably, ACh-treated mice exhibited significantly heightened ILC2 responses following *N. brasiliensis* infection, with higher numbers of total ILC2s (Fig. 6A), significantly increased percentages and numbers of IL-5-producing ILC2s (Fig. 6,B to D) and significantly increased numbers of IL-13-producing ILC2s (Fig. 6,E to G) in the lung compared to control mice. In accordance with increased numbers of IL-5-producing ILC2s, ACh-treated mice exhibited enhanced eosinophil responses, with increased percentages and numbers of total and activated eosinophils in the lung compared to control mice (Fig. 6,H to L). In accordance with increased numbers of IL-13-producing ILC2s, ACh-treated mice exhibited exaggerated goblet cell hyperplasia in the small intestine compared to control mice (Fig. 6,M and N). Associated with enhanced ILC2 responses, ACh-treated mice exhibited significantly lower helminth burden compared to control mice (Fig. 6O). Taken together, these results suggest that ACh may promote anti-helminth immunity through facilitating ILC2 responses and type 2 inflammation.

ILC2-derived ACh is indispensable for optimal ILC2 responses and helminth expulsion

To further analyze the effects of ILC2-derived ACh on anti-helminth innate immune responses, we crossed ChAT^{flox} mice (40) with *Il7r*-Cre mice (14, 41) to generate *Il7r*$^{cre/+}$ *Chat*$^{flox/flox}$ (*Chat*$^{\Delta IL-7R}$) mice. On day 7 of *N. brasiliensis* infection, *Chat*$^{\Delta IL-7R}$ mice exhibited lower numbers of ILC2s in the lung compared to control mice (Fig. 7A), with reduced percentages and numbers of IL-5 and IL-13-producing ILC2s (Fig. 7,B to G). *Chat*$^{\Delta IL-7R}$ mice also exhibited significantly lower numbers of ILC2s in the mLNs compared to control mice (Fig. 7H), with reduced percentages and numbers of IL-5 and IL-13-producing ILC2s (Fig. 7,I to N). Further, *Chat*$^{\Delta IL-7R}$ mice exhibited significantly decreased percentages and numbers of total and activated eosinophils in the lung (Fig. 8,A to E), as well as significantly decreased percentages and numbers of eosinophils in the mLNs compared to control mice (Fig. 8,F to H). Consistent with their impaired ILC2 responses, *Chat*$^{\Delta IL-7R}$ mice exhibited diminished goblet cell responses in the small intestine (Fig. 8,I to J) and significantly higher helminth burden compared to control mice (Fig. 8K). These results suggest that ILC2-derived ACh regulates ILC2 responses and helminth expulsion. Collectively, these data indicate that the ChAT-ACh pathway is an important contributor to optimal ILC2 responses and host defense against helminth infection.

Discussion

Recent studies have shed light on the critical roles of neurotransmitters and neuropeptides in the regulation of innate and adaptive immune responses (8, 9, 42–45). However, the neurotransmitters and neuropeptides that regulate ILC2 responses as well as the cellular sources of these molecules *in vivo*, which may determine the potency and efficiency of their effects, remain incompletely defined. The present study demonstrates that the neurotransmitter ACh plays a critical role in regulating ILC2 responses, and identifies that ILC2s themselves are a previously unrecognized cell type that expresses ChAT and may be a source of ACh. Our results inform a model in which ILC2s express ChAT and utilize the ACh-AChR pathway to promote IL-5 and IL-13 production, type 2 inflammation and anti-helminth immunity (fig. S6).

Different neurotransmitters or neuropeptides and their receptors lead to divergent outcomes in ILC2s. For example, the neuropeptide NMU signals through the $G_{q/11}$-coupled receptor NMUR1, which leads to calcium influx and NFAT signaling, and potently drives ILC2 activation and helminth expulsion (11–13). NE and CGRP signal through their G_s-coupled receptors β2AR and CALCRL/RAMP1, respectively, which lead to cAMP signaling, and inhibit ILC2 activation and anti-helminth immunity (14–17). In the case of AChRs, the mAChR M4 is coupled to $G_{i/o}$ proteins, and M5 is coupled to $G_{q/11}$ proteins (24). nAChRs are pentameric Na^+ ion channels (23). The diverse combination of different alpha and beta subunits assembling heteromeric nAChRs, and with several alpha subunits including α9 and α10 subunits assembling homomeric nAChRs (46), leads to numerous nAChRs that vary in their properties and functions. Given that ILC2s express at least 2 mAChRs plus at least 6 nAChR subunits, using new AChR conditional KO mice to determine which specific receptor subunit pairs of the AChRs play a role in the activation of ILC2s in the context of *N. brasiliensis* infection or exposure to other stimuli will be critical in future studies.

Generation of these new genetic tools will also aid in the analysis of a potential ILC2-ACh autocrine loop and directly test whether the observed effects of ACh administration *in vivo* are direct effects of ACh on ILC2s, rather than indirect effects subsequent to ACh effects on other cells. In this manuscript, we focused on the intestinal phase of *N. brasiliensis* infection. Given that *N. brasiliensis* migrates from the epidermis via blood vessels to the lung, then via the trachea to the intestine, and is eventually expulsed from the intestine, further studies on the role of ILC2 ChAT-ACh pathway in other phases of *N. brasiliensis* infection are needed, as well as in naïve mice and in other models of helminth infection and allergic inflammation.

Although further analysis is required to define how the ACh-AChR pathway is regulated in ILC2s, our data indicate that the ChAT-ACh pathway is induced by the alarmin IL-33, likely dependent on the IL-33R-MyD88 signaling pathway, as the expressions of ChAT in $CD4^+$ T cells and B cells are dependent on the Toll like receptor (TLR)-MyD88 signaling pathway (47, 48). In the nervous system, ACh is stored in vesicles and released after the neuron receives specific neurotransmitter signals. Similar mechanisms were discovered in immune cells—$ChAT^+$ $CD4^+$ T cells release ACh after stimulation with NE, and $ChAT^+$ B cells release ACh after stimulation with cholecystokinin (47, 48). ILC2s respond to several neurotransmitters including NE. Based on these findings, further investigation on the regulation of ACh release from ILC2s is needed.

Pharmacological AChR agonists are already being tested in clinical trials for neurological diseases as well as excessive TNF-α and IL-1β production mediated by macrophage responses (49–54). Given that the ChAT-ACh pathway influences optimal ILC2 responses in both lymphoid tissues and at mucosal barriers in the context of allergen- or helminth-induced type 2 inflammation, ACh and AChR signaling pathways could be potential therapeutic targets to manipulate ILC2 functions in multiple inflammatory and infectious diseases.

Materials and Methods

Study design

The study aimed to identify the role of the ChAT-ACh pathway in regulating ILC2 responses to protect against helminth infection. Experiments included WT mice and transgenic strains. All mice used were between 6 and 16 weeks old and were age- and sex-matched littermates for each experiment. Most of the experiments consisted of enumeration of population frequencies and cell numbers by flow cytometry. We did not use randomization to assign animals to experimental groups. No animals were excluded from the analyses. The investigators were not blinded. The sample size was estimated from preliminary experiments or from reports in the literature. Experimental replication is described in the figure legends.

Mice

C57BL/6 (Jax 664), $ChAT^{BAC}$-eGFP (Jax 7902), $ChAT^{flox}$ (*Chat*^{tm1Jrs}; Jax 16920) and YetCre-13 (*Il13*$^{tm1(YFP/cre)Lky}$; Jax 17353) mice were purchased from The Jackson Laboratories and bred at Weill Cornell Medicine. *Il7r*-Cre (41) were bred at Weill Cornell Medicine. All mice used were between 6 and 16 weeks old and were age- and sex-matched

littermates were used for each experiment. All mice were maintained under specific pathogen-free conditions and were used in accordance with the Institutional Animal Care and Use Committee guidelines at Weill Cornell Medicine.

Helminth infection, *Alternaria* treatment, IL-25, IL-33 and TSLP *in vivo* treatment

For *N. brasiliensis* infection, third-stage larvae (L3) were purified with a Baermann apparatus. After washing three times in PBS, living worms were counted, and 500 purified worms in 250 μl PBS were injected subcutaneously. Tissues were collected on Day 7 post-infection. Collection and enumeration of L5 adult worms was performed as previously described (55). For *T. muris* infection, 200 embryonated eggs were administered by oral gavage. Ceca were collected on Day 3 post-infection. For *Alternaria* treatment, 10 μg *Alternaria alternata* extract (Stallergenes Greer) in 40 μl PBS was intranasally administered for three consecutive days and analyzed one day later.

For IL-25 treatment, 250 ng recombinant IL-25 (R&D Systems) was injected intraperitoneally in a volume of 100 μl daily for three consecutive days and analyzed one day later. For IL-33 treatment, 500 ng recombinant IL-33 (R&D Systems) was injected intraperitoneally in a volume of 100 μl daily for three consecutive days and analyzed one day later. For TSLP treatment, 10 μg recombinant TSLP (Amgen) was injected intraperitoneally in a volume of 100 μl daily for four consecutive days and analyzed one day later.

Isolation of cells from intestinal lamina propria, mesenteric lymph nodes and lung

Small intestine or colon was removed, cleaned from remaining fat tissue and washed in ice-cold PBS (Sigma-Aldrich). Peyer's patches were identified and eliminated. Intestinal tissue was opened longitudinally and washed in ice-cold PBS. Dissociation of epithelial cells was performed by incubation on a shaker at 37 °C in HBSS (Sigma-Aldrich) containing 1% FBS and 5 mM EDTA (Thermo Fisher Scientific) two times for 15 min. After each step, samples were vortexed and the epithelial fraction was filtered through a 100 μm filter. Afterwards, remaining tissue was chopped into small pieces and enzymatic digestion was performed using dispase (0.4 U/ml; Thermo Fisher Scientific), collagenase III (1 mg/ml; Worthington) and DNaseI (20 μg/ml; Sigma-Aldrich). Leukocytes were further enriched by a 40%/80% Percoll (Sigma-Aldrich) gradient. Mesenteric lymph nodes were chopped and incubated in RPMI 1640 medium (Sigma-Aldrich) supplemented with 1% FBS (Sigma-Aldrich), collagenase II (1 mg/mL; Sigma-Aldrich) and DNaseI (20 μg/mL) for 20 min on a shaker at 37°C. Cells were then dissociated using a pasteur pipette, and filtered through a 70 μm cell strainer. Lungs were chopped and incubated in RPMI medium supplemented with Liberase TM (50 μg/mL; Roche) and DNaseI (20 μg/mL) for 1 h at 37°C. The remaining tissues were mashed with a syringe plunger and single cell suspensions were filtered through a 40 μm cell strainer. Leukocytes were then further enriched by 40% Percoll gradient centrifugation and red blood cells were lysed with ACK lysing buffer (Lonza).

Flow cytometry and cell sorting

Mouse single-cell suspensions were incubated on ice with conjugated antibodies in PBS. Dead cells were routinely excluded with Fixable Aqua Dead Cell Stain (Thermo Fisher

Scientific). Lineage-positive cells were excluded by staining for CD3ε (145–2C11), CD5 (53–7.3), FcεRI (Mar-1), F4/80 (BM8), NK1.1 (PK136), B220 (RA3–6B2), CD11b (M1/70) and CD11c (N418). For surface staining, CD45 (30-F11), CD127 (A7R34), CD90.2 (53–2.1), IL-33R (ST2, RMST2–2), KLRG1 (2F1), Siglec F (E50–2440), CCR6 (29–2L17), NKp46 (29A1.4), Ly6G (1A8), CD8α (53–6.7), CD49b (DX5), CD19 (1D3), CD4 (GK1.5), CD25 (PC61.5) were used. Intracellular staining with IL-5 (TRFK5) and IL-13 (eBio13A) antibodies were carried out by using the BD Cytofix/Cytoperm and Perm/Wash solutions. All antibodies used in flow cytometry were purchased from eBioscience, Biolegend or BD Biosciences. Flow cytometry experiments were acquired using a custom configuration Fortessa flow cytometer and the FACS Diva software (BD Biosciences), and analyzed with FlowJo software (TreeStar). Cell sorting experiments were performed using a custom configuration FACSAria cell sorter (BD Biosciences).

In vitro stimulation

Sort-purified small intestinal ILC2s were incubated in complete RPMI-1640 medium (containing 10% FBS, 50 μM 2-mercaptoethanol, 1 mM L-glutamine, 1 mM sodium pyruvate, 100 U/ml penicillin and 100 μg/ml streptomycin) for 4 h at 37 °C and 5% CO_2. Acetylcholine chloride (0.4 mg/ml, Sigma), ipratropium bromide (6 mg/ml) or d-tubocurarine (2 mg/ml), IL-2 (20 ng/ml), IL-7 (20 ng/ml), IL-25 (100 ng/ml), and IL-33 (100 ng/ml) were added if indicated. For intracellular cytokine staining, the culture was supplemented with phorbol 12-myristate 13-acetate (PMA, 100 ng/ml), ionomycin (1 μg/ml) and brefeldin A (10 μg/ml).

In vitro cell culture

Sort-purified small intestinal ILC2s were cultured in complete RPMI-1640 medium at 37°C and 5% CO_2 for three days in the presence of IL-2 (20 ng/mL), IL-7 (20 ng/mL) plus IL-25 (100 ng/mL) or IL-33 (100 ng/mL) if indicated.

Immunofluorescence microscopy

Tissues were harvested in standard fashion and fixed in 4% paraformaldehyde in phosphate-buffered saline (PBS) for 2 hours at 4°C before washing 3 times in PBS. Tissues were then dehydrated overnight at 4°C in 30% sucrose dissolved in PBS. Dehydrated tissues were cryoprotected in OCT medium (Tissue-Tek) and stored at −80°C until sectioning at a thickness of 10 μm using a cryotome (Leica Instruments) and immobilization on Superfrost Plus slides (VWR). Immobilized tissues were then stored at −20°C until immunostaining. Slides were allowed to come to room temperature and excess OCT medium was washed off in PBS and tissue sections were then blocked in PBS with 5% normal goat serum, 5% normal donkey serum (both Jackson Immunoresearch) and 0.1% Triton X-100 (Sigma) for 30 minutes. Tissue sections were then stained with the following primary antibodies diluted in blocking buffer overnight at 4°C: anti-GFP 1:200 (Abcam cat. # 6556), anti-CD3 1:50 (Biolegend clone 17A2), anti-KLRG1 1:50 (eBioscience clone 2F1). Sections were washed 3 times with PBS and then incubated with secondary antibodies (anti-rabbit IgG-Alexa488, anti-hamster IgG-Alexa555, anti-rat IgG-Alexa647, Invitrogen) diluted 1:500 in blocking buffer for 1h at room temperature. Tissue sections were then washed 3 times in PBS, incubated with DAPI (Invitrogen) for 5 minutes prior to a final wash in PBS, and

mounted with Prolong Gold antifade reagent (Invitrogen). Stained sections were imaged on an Olympus FV1000 laser-scanning confocal microscope.

RT–PCR and quantitative PCR

Cells were lysed in RLT buffer (Qiagen). RNA was extracted via RNeasy mini kits (Qiagen), as per the manufacturer's instructions. cDNA was prepared using RevertAid First Strand cDNA Synthesis Kit (Thermo Fisher). Brain and muscle cDNA were used as positive controls for RT-PCR. The primer sequences used for RT-PCR are listed in table S1. Quantitative PCR was performed on cDNA using SYBR green chemistry (Applied Biosystems) and PrimePCR SYBR Green Assay primers (BioRad). Reactions were run on a real-time PCR system (ABI 7500; Applied Biosystems). Samples were normalized to the expression of *Hprt1*.

Administration of acetylcholine *in vivo*

Acetylcholine chloride (Sigma) of 10 mg/kg body weight or the vehicle PBS was injected subcutaneously in a volume of 100 μl twice daily, 10 h apart, during day 2–7 of *N. brasiliensis* infection.

Histology

Proximal intestinal tissues were fixed with 4% paraformaldehyde (bioWORLD), embedded in paraffin, and 5 μm sections stained with PAS combined with Alcian Blue by IDEXX BioResearch. Images were acquired using Nikon Eclipse Ti microscope (Nikon). The number of goblet cells in villus was calculated from the number of goblet cells in more than 10 villi per mouse.

Immunoblotting

ILC2s were sort-purified from small intestine and cultured *in vitro* for 3 days with IL-2 (20 ng/ml), IL-7 (20 ng/ml) and IL-25 (100 ng/ml). Total cell lysate proteins were separated by SDS-PAGE and transferred to nitrocellulose membranes. Membranes were blocked with TBS containing 5% BSA, 0.1% Tween 20. To detect target molecules by immunoblotting, anti–CHRM4 (Abcam 77956) and anti-CHRM5 (Abcam 41171) were used. Appropriate HRP-conjugated secondary reagents were from Jackson Immunoresearch Laboratories.

RNA-seq library preparation

RNA-seq libraries were prepared and sequenced by the Epigenomics Core at Weill Cornell Medicine on an Illumina NextSeq500, producing 50-bp single-end reads. Sequenced reads were demultiplexed using CASAVA v1.8.2 and adapters trimmed using FLEXBAR v2.4 (56).

RNA-seq analysis

Sequenced reads were aligned to the mouse genome GRCm38/mm10 using STAR v2.3.0 (57). Reads counts at the gene level were calculated using Rsubread (58). Normalization for library size and differential expression analysis were performed using DESeq2 (59) v1.18.

Statistical analysis

P value of data sets was determined by unpaired two-sided Student's t-test with 95% confidence interval. Normal distribution was assumed. If equal variances between two groups could not be assumed, Welch's correction was performed. All statistical tests were performed with GraphPad Prism. Error bars depict the SEM.

Supplementary Material

Refer to Web version on PubMed Central for supplementary material.

Acknowledgments:

We thank the Artis lab members for discussion and critical reading of the manuscript.

Funding: This work was supported by the Sackler Brain and Spine Institute Research Grant (to C.C.), the National Heart, Lung, and Blood Institute (5T32 HL134629) and Thomas C. King Pulmonary Fellowship (all to C.N.P.), and the National Institutes of Health (DK126871, AI151599, AI095466, AI095608, AI142213), LEO Foundation, Cure for IBD, Jill Roberts Institute, Sanders Precision Medicine, and Rosanne H. Silbermann Foundation (all to D.A.).

References and Notes:

1. Artis D, Spits H, The biology of innate lymphoid cells. Nature 517, 293–301 (2015). [PubMed: 25592534]
2. Molofsky AB, Savage AK, Locksley RM, Interleukin-33 in Tissue Homeostasis, Injury, and Inflammation. Immunity 42, 1005–1019 (2015). [PubMed: 26084021]
3. Eberl G, Colonna M, Di Santo JP, McKenzie AN, Innate lymphoid cells. Innate lymphoid cells: a new paradigm in immunology. Science 348, aaa6566 (2015). [PubMed: 25999512]
4. Moro K et al. , Innate production of T(H)2 cytokines by adipose tissue-associated c-Kit(+)Sca-1(+) lymphoid cells. Nature 463, 540–544 (2010). [PubMed: 20023630]
5. Neill DR et al. , Nuocytes represent a new innate effector leukocyte that mediates type-2 immunity. Nature 464, 1367–1370 (2010). [PubMed: 20200518]
6. Price AE et al. , Systemically dispersed innate IL-13-expressing cells in type 2 immunity. Proc Natl Acad Sci U S A 107, 11489–11494 (2010). [PubMed: 20534524]
7. Morita H, Moro K, Koyasu S, Innate lymphoid cells in allergic and nonallergic inflammation. J Allergy Clin Immunol 138, 1253–1264 (2016). [PubMed: 27817797]
8. Chu C, Artis D, Chiu IM, Neuro-immune Interactions in the Tissues. Immunity 52, 464–474 (2020). [PubMed: 32187517]
9. Klose CS, Artis D, Neuronal regulation of innate lymphoid cells. Curr Opin Immunol 56, 94–99 (2019). [PubMed: 30530300]
10. Moriyama S, Artis D, Neuronal regulation of group 2 innate lymphoid cells and type 2 inflammation. Adv Immunol 143, 1–9 (2019). [PubMed: 31607366]
11. Cardoso V et al. , Neuronal regulation of type 2 innate lymphoid cells via neuromedin U. Nature 549, 277–281 (2017). [PubMed: 28869974]
12. Klose CSN et al. , The neuropeptide neuromedin U stimulates innate lymphoid cells and type 2 inflammation. Nature 549, 282–286 (2017). [PubMed: 28869965]
13. Wallrapp A et al. , The neuropeptide NMU amplifies ILC2-driven allergic lung inflammation. Nature 549, 351–356 (2017). [PubMed: 28902842]
14. Moriyama S et al. , beta2-adrenergic receptor-mediated negative regulation of group 2 innate lymphoid cell responses. Science 359, 1056–1061 (2018). [PubMed: 29496881]
15. Xu H et al. , Transcriptional Atlas of Intestinal Immune Cells Reveals that Neuropeptide alpha-CGRP Modulates Group 2 Innate Lymphoid Cell Responses. Immunity 51, 696–708 e699 (2019). [PubMed: 31618654]

16. Wallrapp A et al. , Calcitonin Gene-Related Peptide Negatively Regulates Alarmin-Driven Type 2 Innate Lymphoid Cell Responses. Immunity 51, 709–723 e706 (2019). [PubMed: 31604686]
17. Nagashima H et al. , Neuropeptide CGRP Limits Group 2 Innate Lymphoid Cell Responses and Constrains Type 2 Inflammation. Immuinity 51, 682–695 e686 (2019).
18. Lai NY et al. , Gut-Innervating Nociceptor Neurons Regulate Peyer's Patch Microfold Cells and SFB Levels to Mediate Salmonella Host Defense. Cell 180, 33–49 e22 (2020). [PubMed: 31813624]
19. Pinho-Ribeiro FA et al. , Blocking Neuronal Signaling to Immune Cells Treats Streptococcal Invasive Infection. Cell 173, 1083–1097 e1022 (2018). [PubMed: 29754819]
20. Flamar AL et al. , Interleukin-33 Induces the Enzyme Tryptophan Hydroxylase 1 to Promote Inflammatory Group 2 Innate Lymphoid Cell-Mediated Immunity. Immunity 52, 606–619 e606 (2020). [PubMed: 32160524]
21. Loewi O, On the background of the discovery of neurochemical transmission. J Mt Sinai Hosp N Y 24, 1014–1016 (1957). [PubMed: 13481646]
22. Fishman MC, Sir Henry Hallett Dale and acetylcholine story. Yale J Biol Med 45, 104–118 (1972). [PubMed: 4336479]
23. Albuquerque EX, Pereira EF, Alkondon M, Rogers SW, Mammalian nicotinic acetylcholine receptors: from structure to function. Physiol Rev 89, 73–120 (2009). [PubMed: 19126755]
24. Kruse AC et al. , Muscarinic acetylcholine receptors: novel opportunities for drug development. Nat Rev Drug Discov 13, 549–560 (2014). [PubMed: 24903776]
25. Taylor P, Radic Z, The cholinesterases: from genes to proteins. Annu Rev Pharmacol Toxicol 34, 281–320 (1994). [PubMed: 8042853]
26. Sanderson BE, Ogilvie BM, A study of acetylcholinesterase throughout the life cycle of Nippostrongylus brasiliensis. Parasitology 62, 367–373 (1971). [PubMed: 5104618]
27. Sanderson BE, Acetylcholinesterase activity in Nippostrongylus brasiliensis (Nematoda). Comp Biochem Physiol 29, 1207–1213 (1969). [PubMed: 5815784]
28. Klose CS, Artis D, Innate lymphoid cells as regulators of immunity, inflammation and tissue homeostasis. Nat Immunol 17, 765–774 (2016). [PubMed: 27328006]
29. Klose CSN, Artis D, Innate lymphoid cells control signaling circuits to regulate tissue-specific immunity. Cell Res 30, 475–491 (2020). [PubMed: 32376911]
30. Saenz SA et al. , IL25 elicits a multipotent progenitor cell population that promotes T(H)2 cytokine responses. Nature 464, 1362–1366 (2010). [PubMed: 20200520]
31. Diefenbach A, Colonna M, Koyasu S, Development, differentiation, and diversity of innate lymphoid cells. Immunity 41, 354–365 (2014). [PubMed: 25238093]
32. Tallini YN et al. , BAC transgenic mice express enhanced green fluorescent protein in central and peripheral cholinergic neurons. Physiol Genomics 27, 391–397 (2006). [PubMed: 16940431]
33. Liew FY, Girard JP, Turnquist HR, Interleukin-33 in health and disease. Nat Rev Immunol 16, 676–689 (2016). [PubMed: 27640624]
34. Mahlakoiv T et al. , Stromal cells maintain immune cell homeostasis in adipose tissue via production of interleukin-33. Sci Immunol 4, (2019).
35. Spallanzani RG et al. , Distinct immunocyte-promoting and adipocyte-generating stromal components coordinate adipose tissue immune and metabolic tenors. Sci Immunol 4, (2019).
36. Martin NT, Martin MU, Interleukin 33 is a guardian of barriers and a local alarmin. Nat Immunol 17, 122–131 (2016). [PubMed: 26784265]
37. Gause WC, Wynn TA, Allen JE, Type 2 immunity and wound healing: evolutionary refinement of adaptive immunity by helminths. Nat Rev Immunol 13, 607–614 (2013). [PubMed: 23827958]
38. Zhang X et al. , Brain control of humoral immune responses amenable to behavioural modulation. Nature 581, 204–208 (2020). [PubMed: 32405000]
39. Wang H et al. , Nicotinic acetylcholine receptor alpha7 subunit is an essential regulator of inflammation. Nature 421, 384–388 (2003). [PubMed: 12508119]
40. Misgeld T et al. , Roles of neurotransmitter in synapse formation: development of neuromuscular junctions lacking choline acetyltransferase. Neuron 36, 635–648 (2002). [PubMed: 12441053]

41. Schlenner SM et al. , Fate mapping reveals separate origins of T cells and myeloid lineages in the thymus. Immunity 32, 426–436 (2010). [PubMed: 20303297]
42. Godinho-Silva C, Cardoso F, Veiga-Fernandes H, Neuro-Immune Cell Units: A New Paradigm in Physiology. Annu Rev Immunol 37, 19–46 (2019). [PubMed: 30379595]
43. Veiga-Fernandes H, Mucida D, Neuro-Immune Interactions at Barrier Surfaces. Cell 165, 801–811 (2016). [PubMed: 27153494]
44. Huh JR, Veiga-Fernandes H, Neuroimmune circuits in inter-organ communication. Nat Rev Immunol 20, 217–228 (2020). [PubMed: 31848462]
45. Baral P, Udit S, Chiu IM, Pain and immunity: implications for host defence. Nat Rev Immunol 19, 433–447 (2019). [PubMed: 30874629]
46. Hendrickson LM, Guildford MJ, Tapper AR, Neuronal nicotinic acetylcholine receptors: common molecular substrates of nicotine and alcohol dependence. Front Psychiatry 4, 29 (2013). [PubMed: 23641218]
47. Reardon C et al. , Lymphocyte-derived ACh regulates local innate but not adaptive immunity. Proc Natl Acad Sci U S A 110, 1410–1415 (2013). [PubMed: 23297238]
48. Rosas-Ballina M et al. , Acetylcholine-synthesizing T cells relay neural signals in a vagus nerve circuit. Science 334, 98–101 (2011). [PubMed: 21921156]
49. Rosas-Ballina M, Tracey KJ, Cholinergic control of inflammation. J Intern Med 265, 663–679 (2009). [PubMed: 19493060]
50. Jones CK, Byun N, Bubser M, Muscarinic and nicotinic acetylcholine receptor agonists and allosteric modulators for the treatment of schizophrenia. Neuropsychopharmacology 37, 16–42 (2012). [PubMed: 21956443]
51. Freedman R, alpha7-nicotinic acetylcholine receptor agonists for cognitive enhancement in schizophrenia. Annu Rev Med 65, 245–261 (2014). [PubMed: 24111888]
52. Yang T, Xiao T, Sun Q, Wang K, The current agonists and positive allosteric modulators of alpha7 nAChR for CNS indications in clinical trials. Acta Pharm Sin B 7, 611–622 (2017). [PubMed: 29159020]
53. Hoskin JL, Al-Hasan Y, Sabbagh MN, Nicotinic Acetylcholine Receptor Agonists for the Treatment of Alzheimer's Dementia: An Update. Nicotine Tob Res 21, 370–376 (2019). [PubMed: 30137524]
54. de Jonge WJ, Ulloa L, The alpha7 nicotinic acetylcholine receptor as a pharmacological target for inflammation. Br J Pharmacol 151, 915–929 (2007). [PubMed: 17502850]
55. Camberis M, Le Gros G, Urban J Jr., Animal model of Nippostrongylus brasiliensis and Heligmosomoides polygyrus. Curr Protoc Immunol Chapter 19, Unit 19 12 (2003).
56. Dodt M, Roehr JT, Ahmed R, Dieterich C, FLEXBAR-Flexible Barcode and Adapter Processing for Next-Generation Sequencing Platforms. Biology (Basel) 1, 895–905 (2012). [PubMed: 24832523]
57. Dobin A et al. , STAR: ultrafast universal RNA-seq aligner. Bioinformatics 29, 15–21 (2013). [PubMed: 23104886]
58. Liao Y, Smyth GK, Shi W, The Subread aligner: fast, accurate and scalable read mapping by seed-and-vote. Nucleic Acids Res 41, e108 (2013). [PubMed: 23558742]
59. Love MI, Huber W, Anders S, Moderated estimation of fold change and dispersion for RNA-seq data with DESeq2. Genome Biol 15, 550 (2014). [PubMed: 25516281]
60. Roberts LB, Schnoeller C, Berkachy R, et al. Acetylcholine production by group 2 innate lymphoid cells promotes mucosal immunity to helminths. Sci. Immunology, eabd0359 (2021). [PubMed: 33674321]

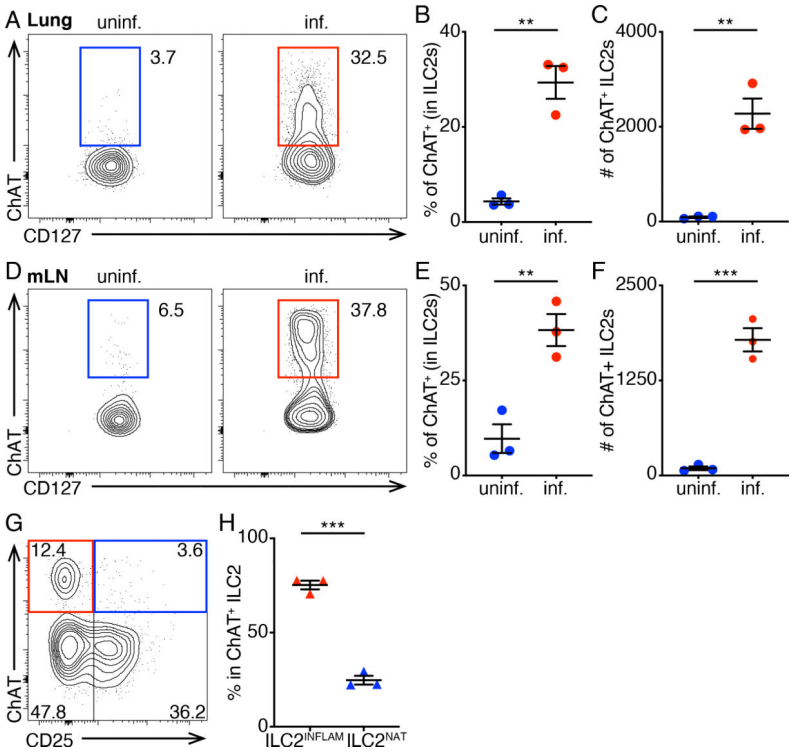

Fig. 1. Upregulated ChAT-eGFP expression in ILC2s following *N. brasiliensis* infection.

(**A** to **F**) Representative flow cytometry plots (A and D), population frequencies (B and E) and numbers (C and F) of ChAT^{+} ILC2s in the lung (A to C) and mLNs (D to F) of uninfected (uninf.) or *N. brasiliensis*-infected (inf.) ChAT^{BAC}-eGFP mice analyzed on Day 7 post-infection, gated on total ILC2s. (**G** and **H**) Representative flow cytometry plot (G) and population frequencies (H) of inflammatory (ILC2^{INFLAM}, red) and natural (ILC2^{NAT}, blue) ILC2s in the mLNs of *N. brasiliensis*-infected ChAT^{BAC}-eGFP mice analyzed on Day 7 post-infection, gated on total ILC2s (G) or ChAT^{+} ILC2s (H). Data are representative of two independent experiments. n = 3 mice per group. Data are mean ± SEM. ** $P < 0.01$, *** $P < 0.001$.

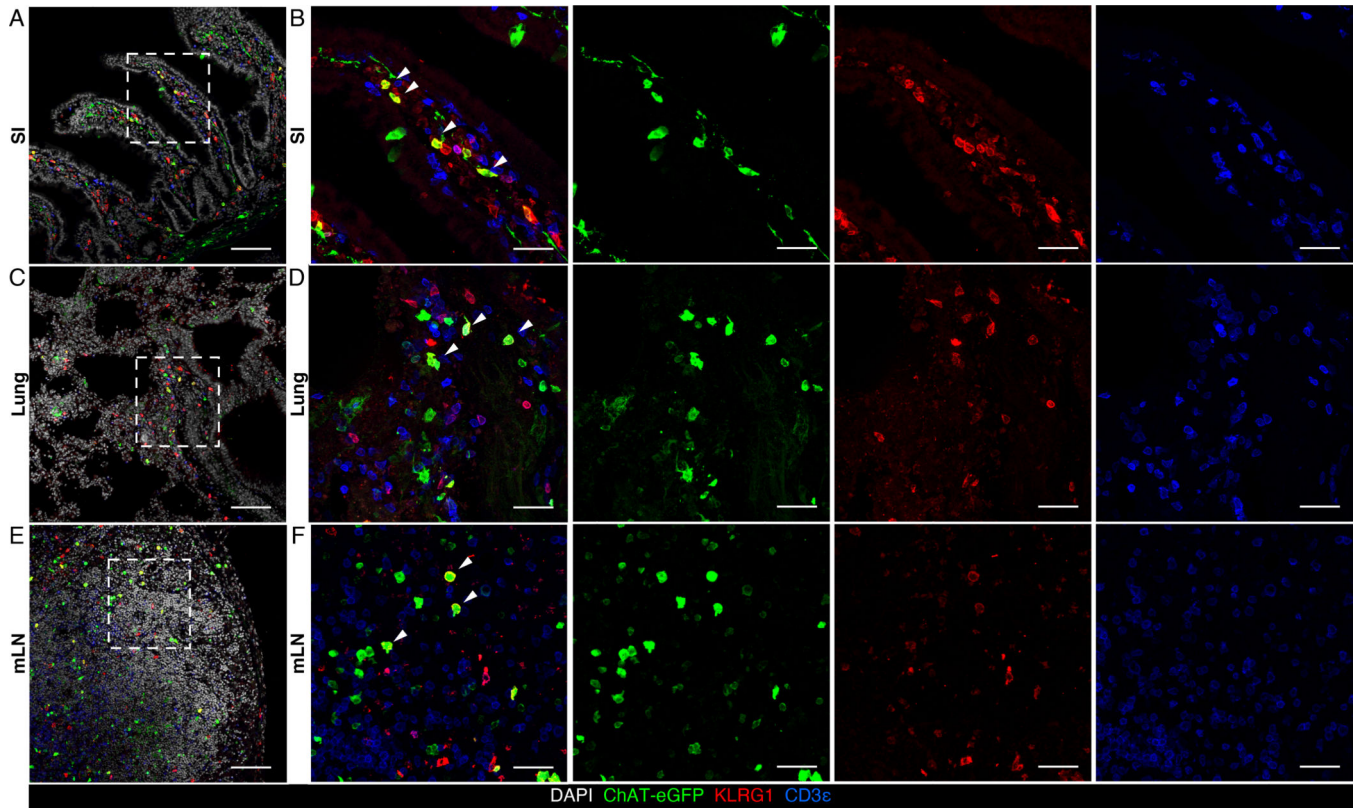

Fig. 2. ChAT-eGFP^{+} ILC2s in the small intestine, mLN and lung of *N. brasiliensis*-infected mice.

(**A** to **F**) Representative sections of small intestine (A and B), lung (C and D), and mLN (E and F) from ChAT-eGFP reporter mice analyzed on Day 7 of *N. brasiliensis* infection, stained for DAPI (white), ChAT-eGFP (green), KLRG1 (red) and CD3ε (blue). Arrows show representative ChAT-eGFP^{+} ILC2s. Data are representative of two independent experiments. Scale bars = 100 μm in (A), (C) and (E), and 30 μm in (B), (D) and (F).

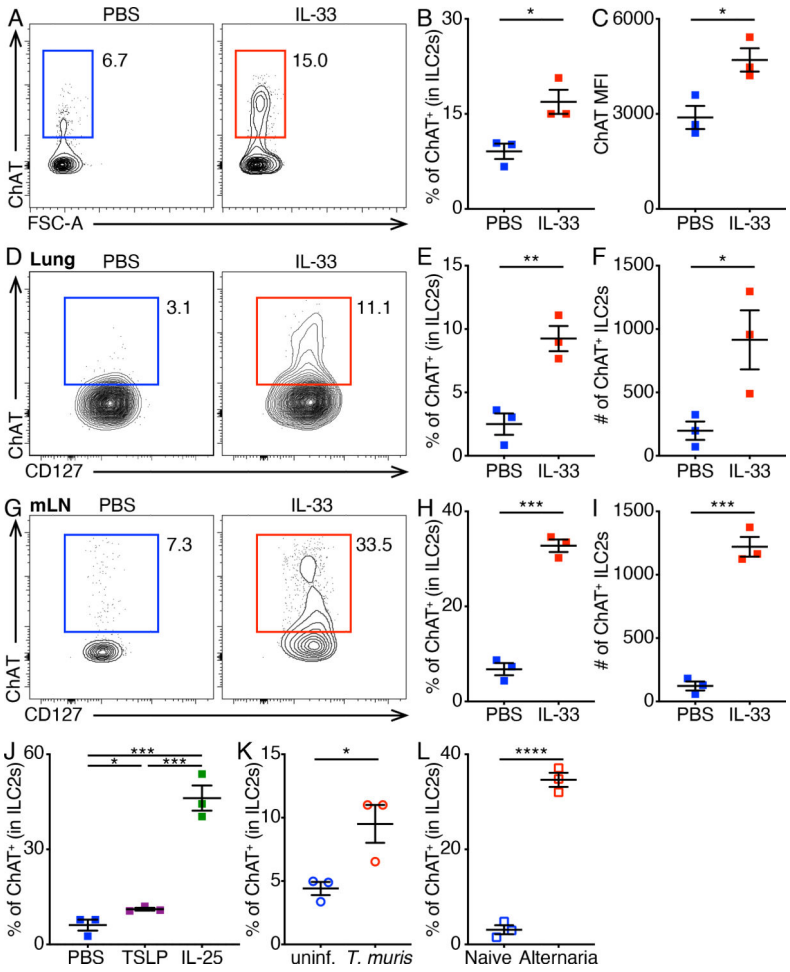

Fig. 3. Upregulated ChAT-eGFP expression in ILC2s after IL-33 treatment.

(**A** to **C**) Representative flow cytometry plots (A), population frequencies (B) and mean fluorescence intensities (C) of ChAT^{+} ILC2s in sort-purified small intestinal ILC2s *in vitro* cultured for 3 days in IL-2 and IL-7 with or without IL-33. (**D** to **I**) Representative flow cytometry plots (D and G), population frequencies (E and H) and numbers (F and I) of ChAT^{+} ILC2s in the lung (D to F) and mLNs (G to I) of PBS or IL-33-treated ChAT^{BAC}-eGFP mice, gated on total ILC2s. (**J** to **L**) Representative population frequencies of ChAT^{+} ILC2s in the mLNs (J), ceca (K) or lung (L) of TSLP or IL-25-treated (J), *T. muris*-infected (K), or *Alternaria*-treated (L) ChAT^{BAC}-eGFP mice, gated on total ILC2s. Data are representative of two independent experiments. n = 3 mice per group. Data are mean ± SEM. * $P < 0.05$, ** $P < 0.01$, *** $P < 0.001$, **** $P < 0.0001$.

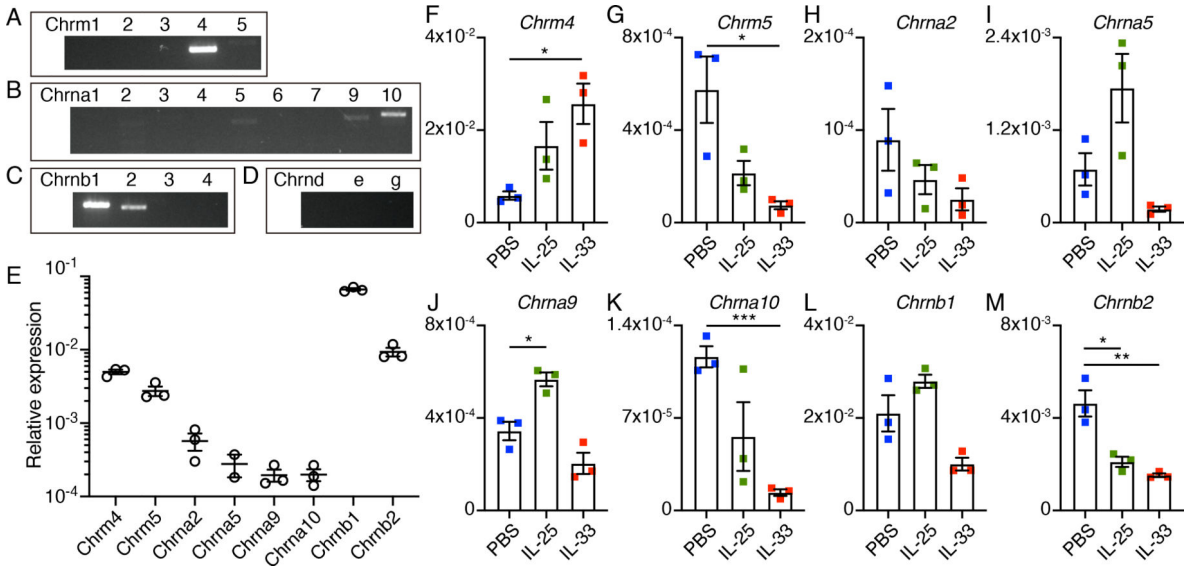

Fig. 4. AChR expression in ILC2s.

(**A** to **D**) RT-PCR analysis of expression of mAChRs (A), α-nAChR subunits (B), β-nAChR subunits (C) and other nAChR subunits (D) in small intestinal ILC2s cultured for 3 days in the presence of IL-2, IL-7 and IL-33. (**E**) qPCR analysis of the expression of candidate AChRs in ILC2s sort-purified from the small intestine, presented relative to Hprt1. Each symbol represents data from ILC2s pooled from 10 mice. (**F** to **M**) qPCR analysis of the expression of candidate mAChRs (F and G), α-nAChR subunits (H to K) and β-nAChR subunits (L and M) in small intestinal ILC2s cultured for 3 days with IL-2 and IL-7 alone (labeled PBS) or additionally supplemented with IL-25 or IL-33, presented relative to Hprt1. Each symbol represents data from sort-purified small intestinal ILC2s pooled from 10 mice in the PBS group, 3 mice in the IL-25 group, and 2 mice in the IL-33 group. Data are mean ± SEM. * $P < 0.05$, ** $P < 0.01$, *** $P < 0.001$.

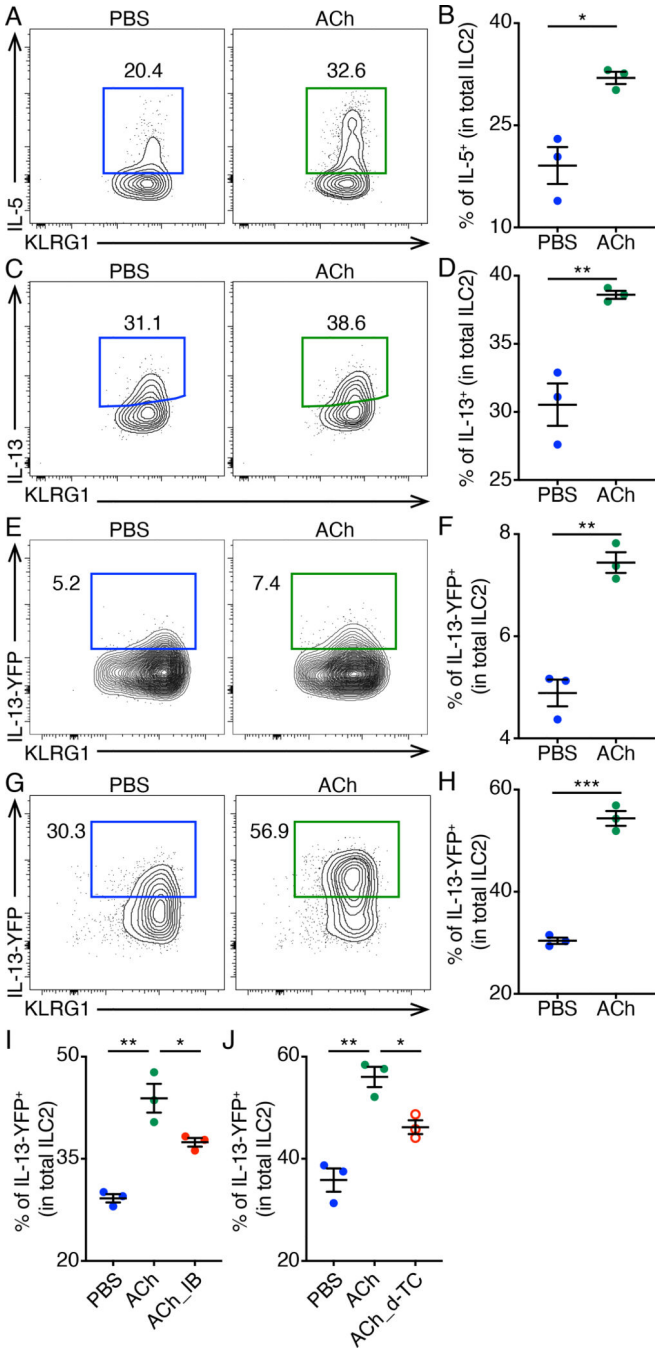

Fig. 5. Increased ILC2 cytokine production after ACh treatment.

(**A** to **D**) Representative flow cytometry plots (A and C) and population frequencies (B and D) of IL-5$^+$ (A and B) and IL-13$^+$ (C and D) ILC2s after 4 h incubation in medium with or without ACh, in the presence of IL-2, IL-7, IL-25, IL-33, PMA and ionomycin, as determined by intracellular cytokine staining. (**E** and **F**) Representative flow cytometry plots (E) and population frequencies (F) of IL-13-YFP$^+$ ILC2s after 4 h incubation in medium with or without ACh. (**G** and **H**) Representative flow cytometry plots (G) and population frequencies (H) of IL-13-YFP$^+$ ILC2s after 4 h incubation in medium with or without

ACh, in the presence of IL-2, IL-7, IL-25 and IL-33. (**I** and **J**) Representative population frequencies of IL-13-YFP$^+$ ILC2s after 4 h incubation in medium with or without ACh and indicated AChR antagonists, in the presence of IL-2, IL-7, IL-25 and IL-33. Data are representative of two independent experiments. n = 3 mice per group. Data are mean ± SEM. * $P < 0.05$, ** $P < 0.01$, *** $P < 0.001$.

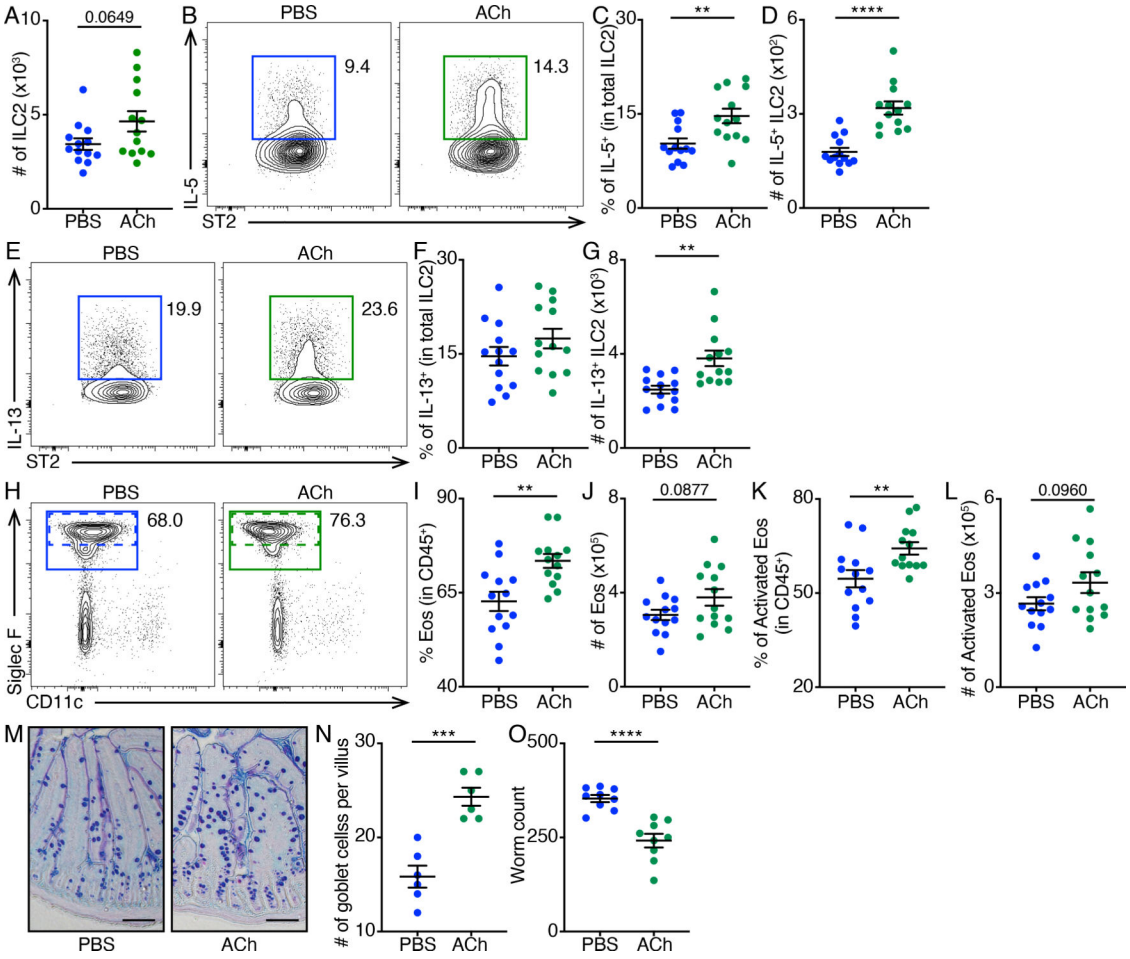

Fig. 6. Enhanced ILC2 responses and accelerated expulsion of *N. brasiliensis* after ACh treatment.

(**A to G**) Numbers of total ILC2s (A), representative flow cytometry plots (B and E), population frequencies (C and F) and numbers (D and G) of IL-5$^+$ (B to D) and IL-13$^+$ (E to G) ILC2s in the lungs of PBS or ACh-treated mice analyzed on Day 7 of *N. brasiliensis* infection. (**H** to **L**) Representative flow cytometry plots (H), population frequencies (I and K) and numbers (J and L) of eosinophils (I and J) and Siglec F^{high} activated eosinophils (K and L) in the lungs of PBS or ACh-treated mice analyzed on Day 7 of *N. brasiliensis* infection. Data are pooled from three independent experiments. n = 13 mice per group. (**M** and **N**) Representative sections (M) and goblet cell numbers (N) of small intestine from PBS or ACh-treated mice analyzed on Day 7 of *N. brasiliensis* infection with periodic acid–Schiff (PAS)–Alcian blue staining. Data are pooled from two independent experiments. n = 6 mice per group. (**O**) Worm counts in the small intestine of PBS or ACh-treated mice analyzed on day 7 of *N. brasiliensis* infection. Data are pooled from two independent experiments. n = 9 mice per group. Data are mean ± SEM. ** $P < 0.01$, *** $P < 0.001$, **** $P < 0.0001$.

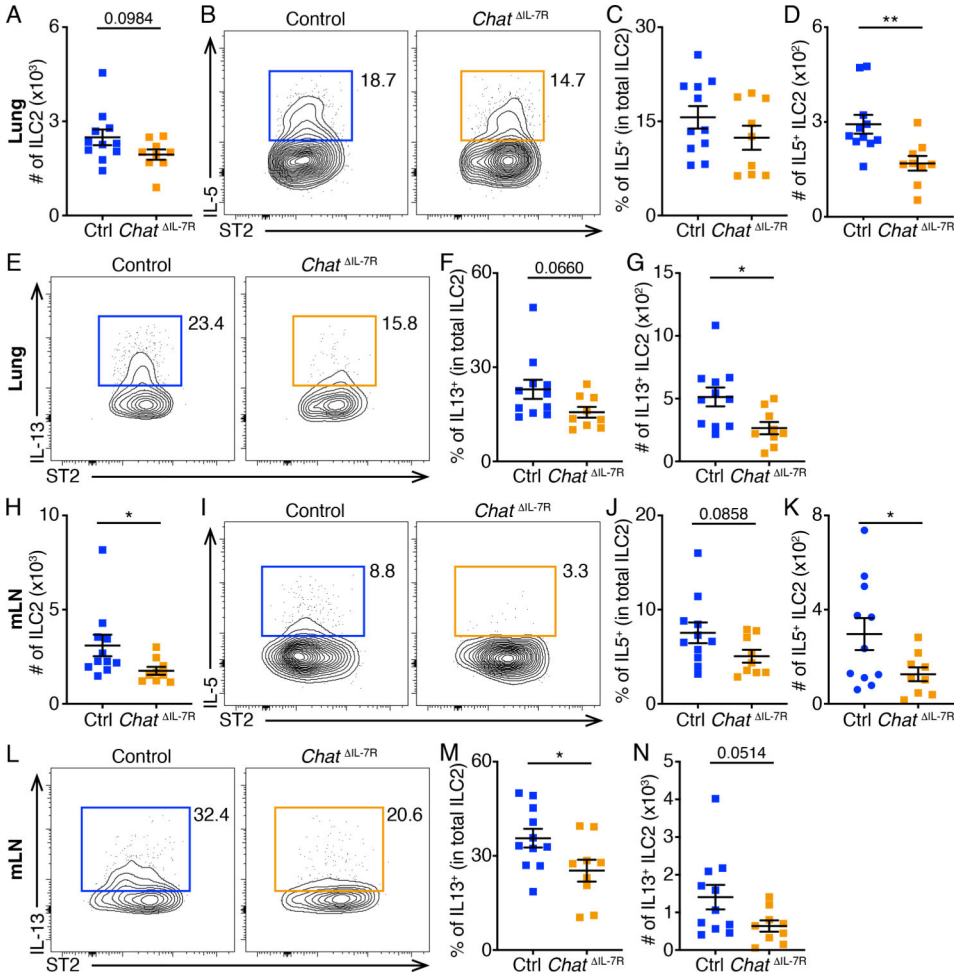

Fig. 7. Defective ILC2 responses in *Chat*$^{\Delta IL-7R}$ mice.

(**A to N**) Numbers of total ILC2s (A and H), representative flow cytometry plots (B, E, I and L), population frequencies (C, F, J and M) and numbers (D, G, K and N) of IL-5^{+} (B to D and I to K) and IL-13^{+} (E to G and L to N) ILC2s in the lung (A to G) and mLNs (H to N) of control or *Chat*$^{\Delta IL-7R}$ mice analyzed on Day 7 of *N. brasiliensis* infection. Data are pooled from three independent experiments. Control, n = 11. *Chat*$^{\Delta IL-7R}$, n = 9. Data are mean ± SEM. * $P < 0.05$, ** $P < 0.01$.

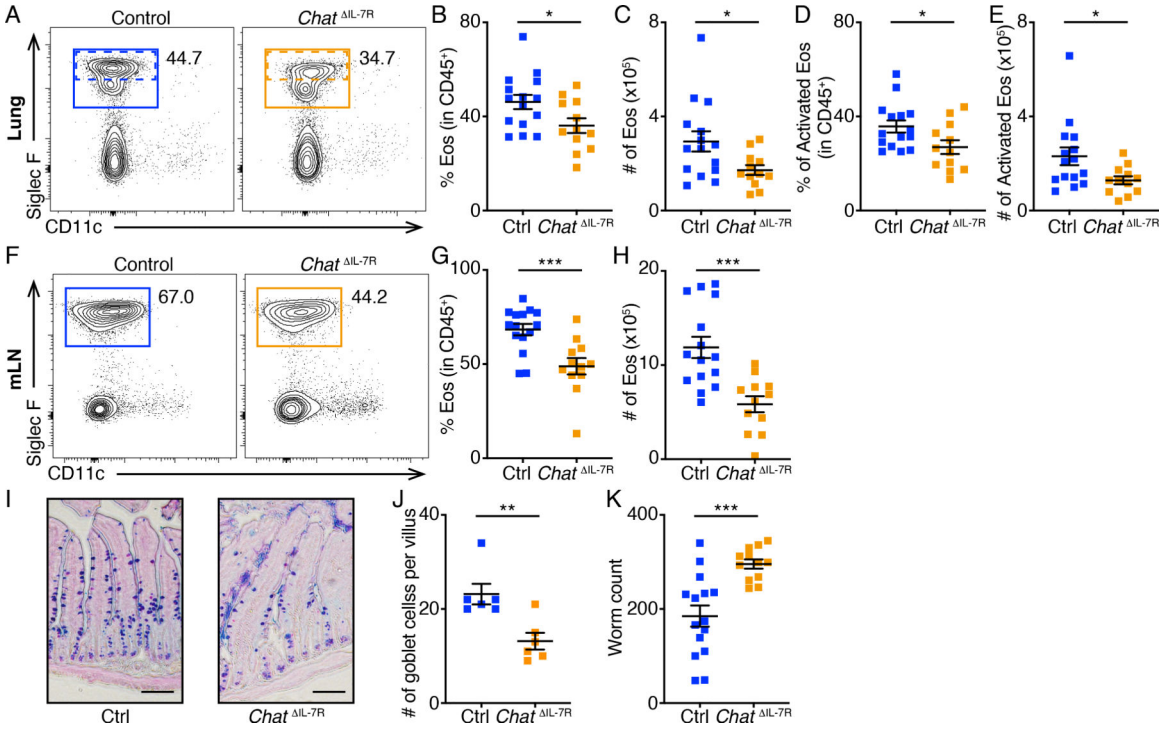

Fig. 8. Defective eosinophil responses and helminth expulsion in *Chat*$^{\Delta IL-7R}$ mice.

(**A** to **H**) Representative flow cytometry plots (A and F), population frequencies (B, D and G) and numbers (C, E and H) of eosinophils (B, C, G and H) and Siglec F^{high} activated eosinophils (D and E) in the lungs (A to E) and mLNs (F to H) of control or *Chat*$^{\Delta IL-7R}$ mice analyzed on Day 7 of *N. brasiliensis* infection. (**I** and **J**) Representative sections (I) and goblet cell numbers (J) of small intestine from control or *Chat*$^{\Delta IL-7R}$ mice analyzed on Day 7 of *N. brasiliensis* infection with periodic acid–Schiff (PAS)–Alcian blue staining. Data are pooled from two independent experiments. n = 6 mice per group. (**K**) Worm counts in the small intestine of control or *Chat*$^{\Delta IL-7R}$ mice analyzed on day 7 of *N. brasiliensis* infection. Data are pooled from four independent experiments. Control, n = 15. *Chat*$^{\Delta IL-7R}$, n = 12. Data are mean ± SEM. * $P < 0.05$, *** $P < 0.001$.